Applications and Applied Mathematics: An International Journal (AAM)

Volume 16 | Issue 1 Article 26

6-2021

Axisymmetric Thermoelastic Response in a Semi-elliptic Plate With Kassir's Nonhomogeneity in the Thickness Direction

Sonal Bhoyar
M.G. College, Armori

Vinod Varghese
Smt. Sushilabai Rajkamalji Bharti Science College, Arni

Lalsingh Khalsa
M.G. College, Armori

Available at
http://pvamu.edu/aam
Appl. Appl. Math.
ISSN: 1932-9466

Applications and Applied Mathematics:
An International Journal
(AAM)

Vol. 16, Issue 1 (June 2021), pp. 481 – 502

Axisymmetric Thermoelastic Response in a Semi-elliptic Plate With Kassir's Nonhomogeneity in the Thickness Direction

[1]Sonal Bhoyar, [2*]Vinod Varghese, and [3]Lalsingh Khalsa

[1,3] Department of Mathematics
M.G. College, Armori
Dist. Gadchiroli, India
[1]sonalwbhoyar@gmail.com;
[3]lalsinghkhalsa@yahoo.com

[2] Department of Mathematics
Smt. Sushilabai Rajkamalji Bharti Science College, Arni
Dist. Yavatmal, India
[2]vino7997@gmail.com

*Corresponding Author

Received: July 8, 2020; Accepted: September 17, 2020

Abstract

The main objective is to investigate the transient thermoelastic reaction in a nonhomogeneous semi-elliptical elastic plate heated sectionally on the upper side of the semi-elliptic region. It has been assumed that the thermal conductivity, calorific capacity, elastic modulus and thermal coefficient of expansion were varying through thickness of the nonhomogeneous material according to Kassir's nonhomogeneity relationship. The transient heat conduction differential equation is solved using an integral transformation technique in terms of Mathieu functions. In these formulations, modified total strain energy is obtained by incorporating the resulting moment and force within the energy term, thus reducing the step of the calculation. The thermal deflection equation derived from the Berger approach is compared with Von Karman approaches, and its maximum normal stresses are determined. The numerical calculation is performed over the metal-metal based composite and graphically portrayed. Furthermore, by applying limiting conditions, the semi-elliptic region can be degenerate into a semi-circular plate. Results reveal that the highest tensile stress exists on the semi-circular core relative to the semi-elliptical core, suggesting the propagation of low heating due to insufficient heat penetration into the elliptic surface.

Keywords: Semi-elliptic plate; Nonhomogeneous material; Heat conduction; Large deflection; Berger approach; von Karman approach; Thermal stress

MSC 2010 No.: 44A10, 33E05, 74E05, 34A25, 74A10, 33C05, 74G50

1. Introduction

In many fields of engineering, semi-elliptic plate structures are widely used as integral structural components. These components are likely to be subjected to various types of static loading or excitation, such as seismic, mechanical, hydrodynamic, blast, aerodynamic, etc., with or without thermal loading. Engineers and scientists worldwide are making unwavering efforts to design and construct economic and efficient structures with a very low probability of failure. In view of this, the thermoelastic behaviour of such structural elements with different boundary and loading conditions should be well known for proper modeling, analysis and design of structural engineers. In plates, the deflections are small compared to the thickness of the elements. This conclusion is based on the assumption that the strain and deflected middle surface components are of marginal significance. Based on linear theory, a large volume of static and dynamic study of thin plates with various boundary and loading conditions has been carried out by many researchers.

In many cases, the spatial properties of the structures combined with the restrictive operating conditions cause large deflections, i.e., deflections of the same size as the thickness of the plate and low for addition to the in-plane dimensions of the structures, even within the elastic limit (proportional limit) of the structural material and therefore generates a nonlinear result. It is worth mentioning that any attempt to restrict the deflections that are relevant to linear theory results in uneconomic systems. Thus, since the deviations are no longer small relative to the width, however significant relative to the in-plane proportions, the intermediate plane stresses must be taken into consideration in deriving the differential equations of thin plate structures. It may be remembered that structural elements undergoing significant deflections (nonlinear deformations) may exhibit strain-hardening or strain-softening behaviour. The benefit of extra strength due to strain-hardening as well as the optimal degree of normal stress frequency can be obtained by carefully integrating and constructing the geometrical features of the systems and their final conditions. In the presence of thermal gradients, the material properties of homogeneous materials are functions of space variables. Therefore, in this case, the determination of dynamic properties of the continuous elastic system must be focused on a nonhomogeneous elastic theory. As a result, during the past decades, there have been many studies based on the large deflection on homogeneous plates, but only a few are mentioned here. Extensive studies on the large deflections of elastic circular plates have been made by Berger's method (Pal (1970a); Pal (1970b); Biswas (1983); Sathyamoorthy and Pandalai (1974)) as well as by von Karman's method (Nowiski (1963); Biswas and Kapoor (1984); Banerjee and Datta (1979)). Berger's approach has some advantages over von Karman's approach since it leads to decoupled equations. However, Nowiski (1963) and Prathap (1970) have pointed out certain inaccuracies in Berger's equations and because of this von Kármán's method should be resorted to until some alternative theory is set forth.

Similarly, during the literature review for nonhomogeneous, it was noted that most of the previous researchers treated the problem theoretically taking the assumption that the thermomechanical material properties change according to the relation of simple power-law $G(z) = G_0\, z^b$ (Kassir (1972)), exponential law $G(z) = G_0\, \exp(az)$ (Buffer (1963b)), power-law $G(z) = G_0(1 + az)^b$ (Buffer (1963a)), and hyperbolic law $G(z) = G_0/(1 + az)$ (Kassir and Sih (1975)). It is also well

known that nonhomogeneous material studies involve a lot of exciting topics, including static and dynamic analyzes, stability analysis, buckling analysis, etc.

With regards to nonhomogenous problems, Tanigawa (1995) reviewed the method of analytical development of thermoelastic problems for nonhomogeneous materials. Jeon et al. (1997) obtained the thermoelastic solution for a medium with Kassir's nonhomogeneous material properties. Sutradhar et al. (2002) used Green's function for deriving the three-dimensional transient heat conduction (diffusion equation) for functionally graded materials. Chiba and Sugano (2007) calculated the statistics of temperature and thermal stress in functionally graded material plates exposed to random external temperatures. Ootao and Tanigawa (2012) obtained the transient thermoelastic solution involving a multilayered hollow circular disk with piecewise power-law nonhomogeneity due to uniform heat supply from inner and outer surfaces. Abd-Alla et al. (2000), El-Naggar et al. (2002), Abd-Alla et al. (2003), and Farhan et al. (2019) have investigated few papers on nonhomogeneous taking into consideration of isotropic and orthotropic type inhomogeneity in solid and multilayered object profiles using a finite-difference model. Edfawy (2016) studied the transient temperature field in the functionally graded plate by solving a nonhomogeneous heat conduction problem for a multilayered plate with linear nonhomogeneous thermal conductivity and different homogeneous heat capacity in each layer. Manthena et al. (2017) determined the temperature distribution, displacement, and thermal stresses in a rectangular plate with inhomogeneous material properties by integral transform method. There are a few more studies reported on this subject. From the literature review, it is noted that none of the researchers has considered Kassir's nonhomogeneity to study the thermally induced instability in the plate. There are a few more heat transfer studies reported, the details of which are cited below. The heat transfer on a stretching porous surface exerted by a magnetic field was studied by Agrawal et al. (2020), and the solution was found numerically using the fourth-order Runga-Kutta shooting technique. Khan et al. (2020a) presented a novel model for oblique channels made of Copper and Aluminum oxide and treated numerically by using coupled shooting and Runge-Kutta scheme. Khan et al. (2020b) studied the thermal transfer, and Joule heating effects on the wire coating process, and evaluated using a dominant numerical technique known as the fourth-order Runge-Kutta method. Tassaddiq et al. (2020) studied heat transfer over an infinite vertical plate in developing an Atangana-Baleanu fractional partial differential equations by making use of the Laplace transform technique. From the literature review, it is noticed that none of the researchers has considered Kassir's nonhomogeneity to study the thermally induced instability on the plate.

The article is organized as follows. In Section 2, the mathematical statement of a transient heat conduction problem in a non-simple medium and its associated thermally induced bending stress is formulated. In Section 3, theoretical solutions of heat conduction, large deflection and stress are expressed in terms of Mathieu function. Section 4 is devoted to the estimates of solutions of the numerical solution is discussed in Section 5. The transition to the nonhomogeneous circular plate as a limiting case is presented in Section 6. Finally, some conclusions are drawn in Section 7.

2. Formulation of the Problem

The elliptic-cylindrical coordinates ξ, η and z are used, as shown in Figure 1.

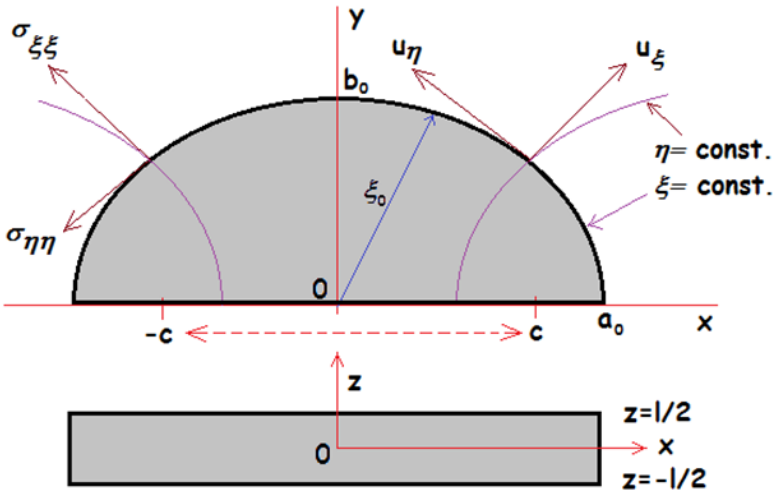

Figure 1. Semi-elliptic plate configuration

The relations between the elliptic coordinate (ξ, η, z) and rectangular coordinate (x, y, z) are expressed as $x = c\cosh\xi\cos\eta$, $y = c\sinh\xi\sin\eta$ and $z = z$, where $2c = 2(a_0^2 - b_0^2)^{1/2}$ is the distance between the focuses of an ellipse. The surfaces of $\xi =$ constant and $\eta =$ constant show an ellipsoid and a hyperboloid, respectively. The side surface of the elliptic plate is represented by $\xi = \xi_0$. The major axis of the ellipse is a_0, the minor axis is $2b_0$, and the eccentricity e is given by $(a_0^2 - b_0^2)^{1/2}/a_0$.

2.1. Heat conduction formulation

It is assumed that a thin semi-elliptic plate is occupying the space $D : \{(\xi, \eta, z) \in R^3 : 0 < \xi < \xi_0, 0 < \eta < \pi, -\ell/2 < z < \ell/2\}$ under transient temperature state having no internal heat source within it, while simply supported at the boundaries as non-rigid. The geometrical parameters are denoted as $\xi \in [0, \xi_0]$, $\eta \in [0, \pi)$ and $z \in (-\ell/2, \ell/2)$, and that can be referred as the elliptic boundary $\xi_0 = \tanh^{-1}(b_0/a_0)$. Initially, the body was kept at zero temperature. The heat conduction differential equation takes the following form,

$$\left\{h^2\left[k\left(\frac{\partial^2}{\partial\xi^2} + \frac{\partial^2}{\partial\eta^2}\right)\right] + \frac{\partial}{\partial z}\left[k\frac{\partial}{\partial z}\right]\right\}T = \rho C_v\frac{\partial T}{\partial t}, \tag{1}$$

in which $T = T(\xi, \eta, z, t)$ is the temperature distribution, $\kappa = k/\rho C_v$ representing thermal diffusivity in which k is the thermal conductivity of the material, ρ is the density, C_v is the calorific capacity and the metric coefficient h is given by $h^2 = 2/[c^2(\cosh 2\xi - \cos 2\eta)]$.

The two-temperature model is one of the non-classical thermoelasticity theories of elastic solids. In this regards, Chen and Gurtin (1968), and Chen et al. (1969) proposed the classification of real

materials into simple and non-simple materials by considering two temperatures (viz., thermodynamic and conductive) and they have shown that the two temperatures are related by

$$\phi = T - b\,\nabla^2 T\,,\ b > 0, \tag{2}$$

in which ϕ is the thermodynamic temperature, T is the conductive temperature and b is the temperature discrepancy factor.

After a few manuscripts, it was noticed that within the context of extended thermodynamics Ciarletta (1996) had developed a theory of thermoelasticity for non-simple material. Quintanilla (2003), Quintanilla (2004), and Sare et al. (2010) proposed some models of non-simple thermoelastic theory with no dissipation of energy. The influence of the dual-phase-lag model of generalized thermoelastic theory without energy dissipation was estimated by Zenkour and Abouelregal (2016). Thus, the thermodynamics and conductive temperatures for non-simple materials are not identical, while they are identical for simple materials. The critical factor that set the two-temperature thermoelasticity theory apart from the classical theory is the material parameter b. Specifically, in the limit as $b \to 0$, $\phi \to T$ and the classical theory, i.e., one-temperature generalised thermoelasticity theory, is recovered. Therefore, in the case of a non-simple medium, Equation (1) maybe written in a non-homogenous semi-elliptic plate for a temperature function that varies along the $z-$ axis as

$$\left(1 + b\frac{\rho C_v(z)}{\lambda(z)}\frac{\partial}{\partial t}\right)\left\{h^2\left[k(z)\left(\frac{\partial^2}{\partial \xi^2} + \frac{\partial^2}{\partial \eta^2}\right)\right] + \frac{\partial}{\partial z}\left[k(z)\frac{\partial}{\partial z}\right]\right\} T = \rho C_v(z)\frac{\partial T}{\partial t}. \tag{3}$$

The boundary and initial conditions for temperature are

$$\phi|_{t=0} = T|_{t=0} = 0, \tag{4}$$

$$T|_{\xi=\xi_0} = 0, \tag{5}$$

$$T|_{z=-\ell/2} = 0\,, \tag{6}$$

$$T|_{z=\ell/2} = [H(\xi) - H(\xi - \xi_0)]\ \sin\ \varpi t \,\text{for}\, t > 0, \tag{7}$$

in which $H(\xi)$ is well-known as the Heaviside function, thermal diffusivity is represented as $\kappa(z) = k(z)/\rho C_v(z)$ with $k(z)$ as the conductivity of the material and $C_v(z)$ as the calorific capacity follows general power-law dependence on the axial coordinate, respectively. This assumption is due to the fact that the ratio of the elasticity matrix to the mass density and thus, the normal frequency or collection of frequencies at which they vibrate would be constant for various heterogeneity parameters for a nonhomogenous material whose mass density sometimes varies according to the power law. To perform a tractable thermoelastic analysis of non-homogeneous material, certain simplifications are therefore required. It is fair to regard Young's nonhomogeneous plate modulus as a durable property (great value in gigapascal unit) that varies along the direction of thickness, with average mass density or a constant value. We have found the mass density and Poisson ratio with a constant value for our convenience in overcoming the mathematical difficulty in finding the exact solution.

We assume that the nonhomogenous property of the thermal conductivity k and the calorific capacity C_v are described in terms of the variable z of the axial coordinate with Kassir's nonhomogeneous material properties as

$$k(z) = k^0(z + \ell/2)^\beta, C_v(z) = C_v^0(z + \ell/2)^\beta, \tag{8}$$

where k^0, C_v^0 and κ^0 are arbitrary constant having the same dimension as k, C_v and κ, respectively. Here β is considered as the material parameter whose combination forms a wide range of nonlinear and continuous profiles to describe the reasonable variation of material constants and thermal expansion coefficients, when the thermal effect is neglected.

Substituting Equation (8) into Equations (3) - (7), one obtains

$$\left(1 + \frac{b}{\kappa_0}\frac{\partial}{\partial t}\right)\left\{h^2\left(\frac{\partial^2}{\partial \xi^2} + \frac{\partial^2}{\partial \eta^2}\right) + \frac{m}{\bar{z}}\frac{\partial}{\partial \bar{z}} + \frac{\partial^2}{\partial \bar{z}^2}\right\}\bar{T} = \frac{1}{\kappa_0}\frac{\partial \bar{T}}{\partial t}, \tag{9}$$

$$\bar{\phi}\big|_{t=0} = \bar{T}\big|_{t=0} = 0, \tag{10}$$

$$\bar{T}\big|_{\xi=\xi_0} = 0, \tag{11}$$

$$\bar{T}\big|_{\bar{z}=0} = 0\,, \tag{12}$$

$$\bar{T}\big|_{\bar{z}=\ell} = 2\pi\left[H(\xi) - H(\xi - \xi_0)\right]\,\sin\,\varpi t \text{ for} t > 0, \tag{13}$$

in which $\bar{z} = z + \ell/2$, $\bar{T} = \bar{T}\,(\,\xi,\,\eta, \bar{z}, t)$ is the temperature distribution.

2.2. Basic equation and stress formulation

The potential energy Bhad et al. (2017) obtained taking into account the strain energy due to thermal bending and stretching in mid-surface during transient temperature change is taken as

$$\begin{aligned} V = \tfrac{1}{2}\iint_s D(z)\left\{(\nabla^2 W)^2 + \tfrac{12}{\ell^2}e_1^2 - 2(1-\upsilon)\left[\tfrac{12}{\ell^2}e_2 + \tfrac{\partial^2 W}{\partial x^2}\tfrac{\partial^2 W}{\partial y^2} - \left(\tfrac{\partial^2 W}{\partial x \partial y}\right)^2\right]\right\} ds \\ - \iint_s \left\{\int_{-\ell/2}^{\ell/2} \tfrac{E(z)\alpha_t(z)}{1-\upsilon}(e_1 - z\nabla^2 W)\,T dz\right\} ds, \end{aligned} \tag{14}$$

where W is the lateral displacement, $D(z)$ is varying flexural rigidity, $E(z)$ is varying Young's modulus, $\alpha_t(z)$ is varying coefficient of thermal expansion in the thickness direction, υ is Poisson ratio, ∇^2 is a Laplacian operator, s the surface under consideration, e_1 is first invariant and e_2 is second invariant, respectively, and is represented as

$$\begin{aligned} &ds = dxdy,\ e_1 = e_x + e_y,\ e_2 = e_x e_y - \gamma_{xy}^2/4, \\ &e_x = \tfrac{\partial u}{\partial x} + \tfrac{1}{2}\left(\tfrac{\partial W}{\partial x}\right)^2,\ e_y = \tfrac{\partial u}{\partial y} + \tfrac{1}{2}\left(\tfrac{\partial W}{\partial y}\right)^2, \\ &\gamma_{xy} = \tfrac{\partial u}{\partial x} + \tfrac{\partial u}{\partial y} + \tfrac{\partial W}{\partial x}\tfrac{\partial W}{\partial y},\ \nabla^2 = \tfrac{\partial^2}{\partial x^2} + \tfrac{\partial^2}{\partial y^2}, \end{aligned} \tag{15}$$

with u and v as the in-plane displacement in cartesian coordinate (x, y). By adding potential energy due to the thermal load and of the foundation reaction to the energy expression of Equation (4)

and neglecting the terms containing the second strain invariant, the modified energy expression becomes

$$V = \frac{1}{2}\iint_s D(z)\left\{(\nabla^2 W)^2 + \frac{12}{\ell^2}e_1^2 - 2(1-\upsilon)\left[\frac{\partial^2 W}{\partial x^2}\frac{\partial^2 W}{\partial y^2} - \left(\frac{\partial^2 W}{\partial x \partial y}\right)^2\right]\right\} dx\, dy \\ -\frac{1}{1-\upsilon}\iint_s \{e_1 N_T - \nabla^2 W M_T\}\, ds, \tag{16}$$

in which M_T is bending resultant moment and N_T is a resultant force as

$$M_T = \int_{-\ell/2}^{\ell/2} \alpha_t(z)E(z)\, z\, T(z)dz, N_T = \int_{-\ell/2}^{\ell/2} \alpha_t(z)E(z)\, T(z)dz. \tag{17}$$

Applying Euler-Lagrange variational principle equations to Equation (2), one yields

$$\nabla^2(\nabla^2 W) - \alpha^2 \nabla^2 W = -12\alpha(\nabla^2 M_T)/\ell^3, \tag{18}$$

in which $\alpha^2 = 12e_1/\ell^2$ is a normalized constant of integration.

The von Karman-type equations with large deflection under thermal load can also be derived from the equations of equilibrium and compatibility as

$$\nabla^2(\nabla^2 F) - [\alpha_t(z)E(z)/(1-\nu)]\nabla^2 N_T = -\,[\ell\, E(z)L(W,W)]/2, \tag{19}$$

$$\nabla^2(\nabla^2 W) + [\alpha_t(z)E(z)/(1-\nu)]\nabla^2 M_T = L(W,F), \tag{20}$$

in which the operator L applied to the functions (W, F) is

$$L(W,F) = \frac{\partial^2 W}{\partial x^2}\frac{\partial^2 F}{\partial y^2} + \frac{\partial^2 W}{\partial y^2}\frac{\partial^2 F}{\partial x^2} - 2\frac{\partial^2 W}{\partial x \partial y}\frac{\partial^2 F}{\partial x \partial y}, \tag{21}$$

and the stress function F which is analogous to the Airy's thermal stress function that satisfies the equation as

$$\nabla^2(\nabla^2)F = -\,\nabla^2 N_T. \tag{22}$$

In order to obtain the solution of large deflection under thermal load, we assume Poisson's ratio υ as a constant value; however, thermal expansion coefficient α_t and Young's modulus E has a power-law dependence on the axial coordinate as

$$\alpha_t(\bar{z}) = \alpha_0(z + \ell/2)^\beta, E(\bar{z}) = E_0(z + \ell/2)^\beta, \tag{23}$$

in which α_0 and E_0 are arbitrary constant having the same dimension as α_t and E, respectively.

2.3. Transient thermal bending stress

The resultant bending moments per unit width is given as

$$M_\xi = -Dh^2\left\{\left(\frac{\partial^2 W}{\partial \xi^2} + \upsilon\frac{\partial^2 W}{\partial \eta^2}\right) - \frac{(1-\upsilon)\sinh 2\xi}{(\cosh 2\xi - \cos 2\eta)}\frac{\partial W}{\partial \xi} + \frac{(1-\upsilon)\sin 2\eta}{(\cosh 2\xi - \cos 2\eta)}\frac{\partial W}{\partial \eta}\right\} - \frac{M_T}{1-\upsilon}, \\ M_\eta = -Dh^2\left\{\left(\upsilon\frac{\partial^2 W}{\partial \xi^2} + \frac{\partial^2 W}{\partial \eta^2}\right) + \frac{(1-\upsilon)\sinh 2\xi}{(\cosh 2\xi - \cos 2\eta)}\frac{\partial W}{\partial \xi} - \frac{(1-\upsilon)\sin 2\eta}{(\cosh 2\xi - \cos 2\eta)}\frac{\partial W}{\partial \eta}\right\} - \frac{M_T}{1-\upsilon}, \\ M_{\xi\eta} = D(1-\upsilon)h^2\left\{\frac{\partial W}{\partial \xi}\sin 2\eta + \frac{\partial W}{\partial \eta}\sinh 2\xi - \frac{\partial^2 W}{\partial \xi \partial \eta}(\cosh 2\xi - \cos 2\eta)\right\}. \tag{24}$$

The maximum bending stresses distributed linearly over the thickness of the plate is

$$\sigma_{\xi\xi} = \left[\frac{M_\xi}{\ell^2/6}\right] \frac{z}{\ell/2},\ \sigma_{\eta\eta} = \left[\frac{M_\eta}{\ell^2/6}\right] \frac{z}{\ell/2},\ \sigma_{\xi\eta} = \left[\frac{M_{\xi\eta}}{\ell^2/6}\right] \frac{z}{\ell/2}. \tag{25}$$

The boundary condition of the clamped plate is given as

$$W(\xi,\eta,t)\,|_{\xi=\xi_0} = \left.\frac{\partial W(\xi,\eta,t)}{\partial\xi}\right|_{\xi=\xi_0} = 0, \quad \text{for all } t. \tag{26}$$

Equations (1) to (26) constitute the mathematical formulation of the considered problem.

3. The Solution to the Problem

3.1. Solution for temperature distribution

Taking the Laplace transform of the Equations (9) and (11) - (13), one gets

$$\left(1+\frac{b}{\kappa_0}p\right)\left\{h^2\left(\frac{\partial^2}{\partial\xi^2}+\frac{\partial^2}{\partial\eta^2}\right)+\frac{m}{\bar{z}}\frac{\partial}{\partial\bar{z}}+\frac{\partial^2}{\partial\bar{z}^2}\right\}\dot{\bar{T}} = \frac{p}{\kappa_0}\dot{\bar{T}}, \tag{27}$$

$$\left.\dot{\bar{T}}\right|_{\xi=\xi_0} = 0, \tag{28}$$

$$\left.\dot{\bar{T}}\right|_{\bar{z}=0} = 0\,, \tag{29}$$

$$\left.\dot{\bar{T}}\right|_{\bar{z}=\ell} = 2\pi\left(\frac{\varpi}{p^2+\varpi^2}\right) f(\xi), \tag{30}$$

where p is transform parameter, and $f(\xi) = H(\xi) - H(\xi-\xi_0)$.

Now, multiply both sides of Equations (27) and (29) - (30), by $Ce_{2n}(\xi,\, q_{2n,m})ce_{2n}(\eta,\, q_{2n,m})$ and integrate with respect to η from 0 to π and with respect to ξ from 0 to ξ_0, and applying the integral transform defined by Gupta (1964), one yields

$$\frac{\partial^2\,\widehat{\dot{\bar{T}}}}{\partial\bar{z}^2}+\frac{m}{\bar{z}}\frac{\partial\,\widehat{\dot{\bar{T}}}}{\partial\bar{z}}-\gamma^2\,\widehat{\dot{\bar{T}}} = 0, \tag{31}$$

$$\left.\widehat{\dot{\bar{T}}}\right|_{\bar{z}=0} = 0, \tag{32}$$

$$\left.\widehat{\dot{\bar{T}}}\right|_{\bar{z}=\ell} = \left(\frac{\varpi}{p^2+\varpi^2}\right) f(q_{2n,m}), \tag{33}$$

where $q_{2n,m}$ is the root of the transcendental equation $Ce_{2n}(a,\, q) = 0$, $ce_{2n}(\eta,\, q)$ is a Mathieu function, $Ce_{2n}(\xi,\, q)$ is a modified Mathieu function, $\lambda^2_{2n,m} = 4q_{2n,m}/c^2$,$\gamma^2 = \lambda^2_{2n,m} + \Lambda^2$, $\Lambda^2 = (p/\kappa_0)/[1 + (b/\kappa_0)p]$, and

$$f(q_{2n,m}) = \int_0^{\xi_0}\int_0^{\pi} f(\xi,\eta)(\cosh 2\xi - \cos 2\eta)Ce_{2n}(\xi, q_{2n,m})ce_{2n}(\eta, q_{2n,m})d\xi d\eta.$$

It is convenient to first introduce a new dependent variable $\widehat{\dot{\theta}}$ in Equations (31) to (33) as

$$\widehat{\dot{T}} = \bar{z}^{(1-m)/2}\ \widehat{\dot{\theta}}, \tag{34}$$

$$\frac{\partial^2\ \widehat{\dot{\theta}}}{\partial\bar{z}^2} + \frac{1}{\bar{z}}\frac{\partial\ \widehat{\dot{\theta}}}{\partial\bar{z}} - \left(\gamma^2 + \frac{\beta^2}{\bar{z}^2}\right)\widehat{\dot{\theta}} = 0, \tag{35}$$

$$\left.\widehat{\dot{\theta}}\right|_{\bar{z}=0} = 0\,, \tag{36}$$

$$\left.\widehat{\dot{\theta}}\right|_{\bar{z}=\ell} = \frac{1}{\ell^\beta}\left(\frac{\varpi}{p^2+\varpi^2}\right) f(q_{2n,m}), \tag{37}$$

where

$$\beta = (m-1)/2.$$

The solution of Equation (35) is obtained as

$$\widehat{\dot{\theta}} = C_1 I_\beta(\gamma z) + C_2 K_\beta(\gamma z), \tag{38}$$

in which I_β and K_β are modified Bessel functions of the first and second kind of order β, respectively.

The arbitrary constants C_1 and C_2 given in Equation (38), can be determined by using Equations (36) and (37) as

$$\begin{aligned} C_1 &= \tfrac{1}{\ell^\beta G(p)}\left(\tfrac{\varpi}{p^2+\varpi^2}\right) f(q_{2n,m})K_\beta(0), \\ C_2 &= \tfrac{-1}{\ell^\beta G(p)}\left(\tfrac{\varpi}{p^2+\varpi^2}\right) f(q_{2n,m})I_\beta(0), \end{aligned} \tag{39}$$

where

$$G(p) = I_\beta(\gamma\ell)K_\beta(0) - I_\beta(0)K_\beta(\gamma\ell). \tag{40}$$

Applying inversion Mathieu transformation, one gets

$$\begin{aligned} \dot{\bar{\theta}} = {} & \textstyle\sum_{n=0}^{\infty}\sum_{m=1}^{\infty}\frac{1}{\ell^\beta G(p)}\left(\frac{\varpi}{p^2+\varpi^2}\right) f(q_{2n,m})[K_\beta(0)\, I_\beta(\gamma z) - I_\beta(0)\, K_\beta(\gamma z)] \\ & \times Ce_{2n}(\xi, q_{2n,m})ce_{2n}(\eta, q_{2n,m}). \end{aligned} \tag{41}$$

Applying inversion Laplace transformation, one gets

$$\bar{\theta} = \frac{1}{2\pi i}\int_{\psi-i\infty}^{\psi+i\infty} \dot{\bar{\theta}}\, e^{pt}\, dt, \tag{42}$$

where ψ is a real number such that all the poles of the integrand in Equation (42) lie on the left of the line $p = \psi$ in the complex plane p.

Now substituting $p = i\varphi$ and using properties of Bessel functions, one obtains

$$G(i\varphi) = G(-i\varphi) = \pi\,[J_\beta(0)\,Y_\beta(\gamma'\ell) - J_\beta(\gamma'\ell)\,Y_\beta(0)]/2, \tag{43}$$

where

$$\gamma'^2 = \lambda_{2n,m}^2 + (\varphi/\kappa_0)/[1 + (b/\kappa_0)\varphi].$$

Since $G(i\varphi) = G(-i\varphi)$, the roots of the Equation (58) maybe denoted by $\pm iR_s\,(s = 1, 2, ...)$.

The poles of the integrand in Equation (42) are at $\pm\, i\,\varpi$ and $\pm iR_s\,(s = 1, 2, ...)$. Applying the Residue Theorem to inversion integral in Equation (42), one obtains

$$\begin{aligned}\bar{\theta}(\xi,\eta,z,t) = {} & \textstyle\sum_{n=0}^{\infty}\sum_{m=1}^{\infty} \frac{f(q_{2n,m})}{(3\ell/2)^\beta}\left\{\frac{F(\gamma\,\varpi)}{F(\gamma'\varpi)}\,\sin(\varpi t) + \sum_{s=1}^{\infty}\left(\frac{\pi\varpi}{\varpi^2-R_s^2}\right)\frac{H(R_s)}{M(R_s)}\sin(R_s t)\right\} \\ & \times Ce_{2n}(\xi, q_{2n,m})ce_{2n}(\eta, q_{2n,m}),\end{aligned} \tag{44}$$

where

$$F(\gamma\,\varpi) = J_\beta(0)\,Y_\beta(\gamma\,\varpi) - J_\beta(\gamma\,\varpi)\,Y_\beta(0),$$

$$H(R_s) = J_\beta(\gamma' R_s)\,J_\beta(0)\{J_\beta(0)\,Y_\beta(\gamma\,R_s) - J_\beta(\gamma\,R_s)\,Y_\beta(0)\}\,R_s,$$

$$M(R_s) = [J_\beta(\gamma' R_s)]^2 - [J_\beta(0)]^2.$$

Finally using the dependent variable defined in Equation (32), it results in

$$\begin{aligned}T(\xi,\eta,z,t) = {} & \textstyle\sum_{n=0}^{\infty}\sum_{m=1}^{\infty} \frac{f(q_{2n,m})}{(\varpi^2-R_s^2)^\beta}\left\{\frac{F(\gamma\varpi)}{F(\gamma'\varpi)}\,\sin(\varpi t) + \sum_{s=1}^{\infty}\left(\frac{\pi\varpi}{\varpi^2-R_s^2}\right)\frac{H(R_s)}{M(R_s)}\sin(R_s t)\right\} \\ & \times [z+\ell/2]^{(1-m)/2} Ce_{2n}(\xi, q_{2n,m})ce_{2n}(\eta, q_{2n,m}).\end{aligned} \tag{45}$$

The above function, which is given in Equation (45), represents the temperature at every instance and at all points of the non-homogenous semi-elliptic plate under the influence of ramp-type boundary conditions.

3.2. The solution for thermal displacement and stresses

Substituting Equation (45) into Equation (17), one arrives at the resultant moment and resultant force as

$$\begin{aligned}M_T = {} & \textstyle\sum_{n=0}^{\infty}\sum_{m=1}^{\infty} \frac{\alpha_0 E_0 f(q_{2n,m})\ell^{(5-m+4\beta)}\,(-m+1+4\,\beta)}{(\varpi^2-R_s^2)^\beta(m-5-4\,\beta)(m-3-4\,\beta)}\left\{\frac{F(\gamma\,\varpi)}{F(\gamma'\varpi)}\,\sin(\varpi t)\right. \\ & \left. + \sum_{s=1}^{\infty}\left(\frac{\pi\varpi}{\varpi^2-R_s^2}\right)\frac{H(R_s)}{M(R_s)}\sin(R_s t)\right\} Ce_{2n}(\xi, q_{2n,m})ce_{2n}(\eta, q_{2n,m}),\end{aligned} \tag{46}$$

$$N_T = \sum_{n=0}^{\infty}\sum_{m=1}^{\infty} \frac{2\alpha_0 E_0 f(q_{2n,m})\ell^{(-m+3+4\beta)}}{(\varpi^2-R_s^2)^{\beta}(-m+3+4\,\beta)} \left\{ \frac{F(\gamma\,\varpi)}{F(\gamma'\varpi)} \sin(\varpi t) + \sum_{s=1}^{\infty}\left(\frac{\pi\varpi}{\varpi^2-R_s^2}\right)\frac{H(R_s)}{M(R_s)}\sin(R_s t)\right\} Ce_{2n}(\xi, q_{2n,m})ce_{2n}(\eta, q_{2n,m}). \tag{47}$$

Substituting Equation (46) into Equation (18), one obtains the thermal deflection as

$$W = \sum_{n=0}^{\infty}\sum_{m=1}^{\infty} A'\ \bar{z}^{(1-m)/2}\left\{\frac{F(\gamma\,\varpi)}{F(\gamma'\varpi)}\sin(\varpi t) + \sum_{s=1}^{\infty}\left(\frac{\pi\varpi}{\varpi^2-R_s^2}\right)\frac{H(R_s)}{M(R_s)}\sin(R_s t)\right\} \times Ce_{2n}(\xi, q_{2n,m})ce_{2n}(\eta, q_{2n,m}), \tag{48}$$

where

$$\begin{aligned} A' = -\sum_{n=0}^{\infty}\sum_{m=1}^{\infty} & \frac{12\,\alpha_0 E_0 f(q_{2n,m})\ell^{(5-m+4\beta)}\,(-m+1+4\,\beta)}{\ell^3(\varpi^2-R_s^2)^{\beta}(m-5-4\,\beta)(m-3-4\,\beta)} \\ & \times Ce_{2n}(\xi, q_{2n,m})ce_{2n}(\eta, q_{2n,m}) / \left\langle \{Ce''_{2n}(\xi, q_{2n,m})ce''_{2n}(\eta, q_{2n,m}) \right. \\ & \times [-1+(m-1)/2](1-m)\,[z+\ell/2]^{-3-m/2}/2\} \\ & \left. -\alpha^2\{Ce_{2n}(\xi, q_{2n,m})ce_{2n}(\eta, q_{2n,m})[z+\ell/2]^{(1-m)/2}\}\right\rangle. \end{aligned}$$

Substituting Equation (48) into Equation (24), one obtains resultant bending moments per unit width as

$$\begin{aligned} M_\xi = Dh^2 \sum_{n=0}^{\infty}\sum_{m=1}^{\infty} & \left\{\frac{F(\gamma\,\varpi)}{F(\gamma'\varpi)}\sin(\varpi t) + \sum_{s=1}^{\infty}\left(\frac{\pi\varpi}{\varpi^2-R_s^2}\right)\frac{H(R_s)}{M(R_s)}\sin(R_s t)\right\} \left\langle [z+\ell/2]^{(1-m)/2}A' \right. \\ & \times \{-[Ce''_{2n}(\xi, q_{2n,m})ce_{2n}(\eta, q_{2n,m}) + \upsilon Ce_{2n}(\xi, q_{2n,m})ce''_{2n}(\eta, q_{2n,m})] \\ & + \frac{(1-\upsilon)\sinh 2\xi}{(\cosh 2\xi-\cos 2\eta)} Ce'_{2n}(\xi, q_{2n,m})ce_{2n}(\eta, q_{2n,m}) - \frac{(1-\upsilon)\sin 2\eta}{(\cosh 2\xi-\cos 2\eta)} \\ & \left. \times Ce_{2n}(\xi, q_{2n,m})ce'_{2n}(\eta, q_{2n,m})\,\} + A_{2nm}\, Ce_{2n}(\xi, q_{2n,m})ce_{2n}(\eta, q_{2n,m})\right\rangle, \end{aligned} \tag{49}$$

$$\begin{aligned} M_\eta = Dh^2 \sum_{n=0}^{\infty}\sum_{m=1}^{\infty} & \left\{\frac{F(\gamma\,\varpi)}{F(\gamma'\varpi)}\sin(\varpi t) + \sum_{s=1}^{\infty}\left(\frac{\pi\varpi}{\varpi^2-R_s^2}\right)\frac{H(R_s)}{M(R_s)}\sin(R_s t)\right\} \left\langle [z+\ell/2]^{(1-m)/2}A' \right. \\ & \times \{-[\upsilon Ce''_{2n}(\xi, q_{2n,m})ce_{2n}(\eta, q_{2n,m}) + Ce_{2n}(\xi, q_{2n,m})ce''_{2n}(\eta, q_{2n,m})] \\ & - \frac{(1-\upsilon)\sinh 2\xi}{(\cosh 2\xi-\cos 2\eta)} Ce'_{2n}(\xi, q_{2n,m})ce_{2n}(\eta, q_{2n,m}) + \frac{(1-\upsilon)\sin 2\eta}{(\cosh 2\xi-\cos 2\eta)} \\ & \left. \times Ce_{2n}(\xi, q_{2n,m})ce'_{2n}(\eta, q_{2n,m})\,\} + A_{2nm}\, Ce_{2n}(\xi, q_{2n,m})ce_{2n}(\eta, q_{2n,m})\right\rangle, \end{aligned} \tag{50}$$

$$\begin{aligned} M_{\xi\eta} = D(1-\upsilon)h^2 \sum_{n=0}^{\infty}\sum_{m=1}^{\infty} & A'\left\{\frac{F(\gamma\,\varpi)}{F(\gamma'\varpi)}\sin(\varpi t) + \sum_{s=1}^{\infty}\left(\frac{\pi\varpi}{\varpi^2-R_s^2}\right)\frac{H(R_s)}{M(R_s)}\sin(R_s t)\right\} [z+\ell/2]^{(1-m)/2} \\ & \times \{\ \sin 2\eta\, Ce'_{2n}(\xi, q_{2n,m})ce_{2n}(\eta, q_{2n,m}) + \sinh 2\xi Ce_{2n}(\xi, q_{2n,m}) \\ & \times ce'_{2n}(\eta, q_{2n,m}) - (\cosh 2\xi - \cos 2\eta)Ce'_{2n}(\xi, q_{2n,m})ce'_{2n}(\eta, q_{2n,m})\,\}, \end{aligned} \tag{51}$$

in which

$$A_{2nm} = \frac{\alpha_0 E_0 f(q_{2n,m})\ell^{(5-m+4\beta)}\,(-m+1+4\,\beta)}{(1-\upsilon)(\varpi^2-R_s^2)^{\beta}(m-5-4\,\beta)(m-3-4\,\beta)}.$$

Substituting Equations (49) - (51) into Equation (25), one obtains maximum normal bending stresses as

$$\begin{aligned}\sigma_{\xi\xi} = \tfrac{12D\,h^2 z}{\ell^3} \sum_{n=0}^{\infty}\sum_{m=1}^{\infty} \Big\{ \tfrac{F(\gamma\,\varpi)}{F(\gamma'\varpi)}\,\sin(\varpi t) \\ + \sum_{s=1}^{\infty}\left(\tfrac{\pi\varpi}{\varpi^2-R_s^2}\right)\tfrac{H(R_s)}{M(R_s)}\sin(R_s t)\Big\}\big\langle [z+\ell/2]^{(1-m)/2}A' \\ \times\{-[Ce''_{2n}(\xi,q_{2n,m})ce_{2n}(\eta,q_{2n,m}) + \upsilon Ce_{2n}(\xi,q_{2n,m})ce''_{2n}(\eta,q_{2n,m})] \\ +\tfrac{(1-\upsilon)\sinh 2\xi}{(\cosh 2\xi-\cos 2\eta)}Ce'_{2n}(\xi,q_{2n,m})ce_{2n}(\eta,q_{2n,m}) - \tfrac{(1-\upsilon)\sin 2\eta}{(\cosh 2\xi-\cos 2\eta)} \\ \times Ce_{2n}(\xi,q_{2n,m})ce'_{2n}(\eta,q_{2n,m})\,\} + A_{2nm}\,Ce_{2n}(\xi,q_{2n,m})ce_{2n}(\eta,q_{2n,m})\big\rangle\,,\end{aligned} \tag{52}$$

$$\begin{aligned}\sigma_{\eta\eta} = \tfrac{12D\,h^2 z}{\ell^3} \sum_{n=0}^{\infty}\sum_{m=1}^{\infty} \Big\{ \tfrac{F(\gamma\,\varpi)}{F(\gamma'\varpi)}\,\sin(\varpi t) \\ + \sum_{s=1}^{\infty}\left(\tfrac{\pi\varpi}{\varpi^2-R_s^2}\right)\tfrac{H(R_s)}{M(R_s)}\sin(R_s t)\Big\}\big\langle [z+\ell/2]^{(1-m)/2}A' \\ \times\{-[\upsilon Ce''_{2n}(\xi,q_{2n,m})ce_{2n}(\eta,q_{2n,m}) + Ce_{2n}(\xi,q_{2n,m})ce''_{2n}(\eta,q_{2n,m})] \\ -\tfrac{(1-\upsilon)\sinh 2\xi}{(\cosh 2\xi-\cos 2\eta)}Ce'_{2n}(\xi,q_{2n,m})ce_{2n}(\eta,q_{2n,m}) + \tfrac{(1-\upsilon)\sin 2\eta}{(\cosh 2\xi-\cos 2\eta)} \\ \times Ce_{2n}(\xi,q_{2n,m})ce'_{2n}(\eta,q_{2n,m})\,\} + A_{2nm}\,Ce_{2n}(\xi,q_{2n,m})ce_{2n}(\eta,q_{2n,m})\big\rangle\,,\end{aligned} \tag{53}$$

$$\begin{aligned}\sigma_{\xi\eta} = \tfrac{12D(1-\upsilon)h^2 z}{\ell^3} \sum_{n=0}^{\infty}\sum_{m=1}^{\infty} A' \Big\{ \tfrac{F(\gamma\,\varpi)}{F(\gamma'\varpi)}\,\sin(\varpi t) \\ + \sum_{s=1}^{\infty}\left(\tfrac{\pi\varpi}{\varpi^2-R_s^2}\right)\tfrac{H(R_s)}{M(R_s)}\sin(R_s t)\Big\}\,[z+\ell/2]^{(1-m)/2} \\ \times\{\sin 2\eta\,Ce'_{2n}(\xi,q_{2n,m})ce_{2n}(\eta,q_{2n,m}) + \sinh 2\xi Ce_{2n}(\xi,q_{2n,m}) \\ \times ce'_{2n}(\eta,q_{2n,m}) - (\cosh 2\xi-\cos 2\eta)Ce'_{2n}(\xi,q_{2n,m})ce'_{2n}(\eta,q_{2n,m})\,\}\,.\end{aligned} \tag{54}$$

From Equation (22) and (47), the following thermal stress function is obtained as

$$\begin{aligned}F = \sum_{n=0}^{\infty}\sum_{m=1}^{\infty} B_{2mn}\sin[(1-m)\,z]\Big\{ \tfrac{F(\gamma\,\varpi)}{F(\gamma'\varpi)}\,\sin(\varpi t) \\ + \sum_{s=1}^{\infty}\left(\tfrac{\pi\varpi}{\varpi^2-R_s^2}\right)\tfrac{H(R_s)}{M(R_s)}\sin(R_s t)\Big\}\,Ce_{2n}(\xi,q_{2n,m})ce_{2n}(\eta,q_{2n,m}),\end{aligned} \tag{55}$$

in which

$$\begin{aligned}B_{2mn} = \sum_{n=0}^{\infty}\sum_{m=1}^{\infty}\tfrac{2\alpha_0 E_0 f(q_{2n,m})\ell^{(-m+3+4\beta)}}{h^2(1-m)^2(\varpi^2-R_s^2)^{\beta}(-m+3+4\,\beta)} \\ \times\left(\tfrac{Ce_{2n}(\xi,q_{2n,m})ce_{2n}(\eta,q_{2n,m})}{\sin[(1-m)\,z]Ce''_{2n}(\xi,q_{2n,m})ce''_{2n}(\eta,q_{2n,m})}\right).\end{aligned}$$

We assume now that W is identical to that taken in Equation (48), and putting W and F from Equation (55) into Equation (20), one arrives at the desired von Karman-type large deflection on a nonhomogeneous semi-elliptic elastic plate undergoing ramp-type heating on the upper face of the semi-elliptic region. The constant term A' seems to be quite lengthy; therefore, it is not written here for the sake of brevity, but the same is plotted in the deflection graph.

4. Numerical Results, Discussion and Remarks

For the sake of simplicity of calculation, we introduce the following dimensionless values,

$$\begin{aligned}&\bar{\xi} = \xi/\xi_0,\ \bar{z} = [z-(-\ell/2)]/\xi_0,\ e = c/\xi_0,\ \bar{h}^2 = h^2\xi_0^2, \\ &\tau = \kappa\,t/\xi_0^2,\ \overline{T} = T/T_0,\ \bar{W} = W/[12(1+\upsilon)]\alpha_t T_0\xi_0, \\ &\bar{M}_{ij} = M_{ij}/Ea_0^3,\ \bar{\sigma}_{ij} = \sigma_{ij}/E\alpha_t T_0\,(i,j=\xi,\eta).\end{aligned} \tag{56}$$

The mechanical material properties taken by Hata (1985) are considered for a semi-elliptic plate is shown in Table 1.

Table 1. Thermo-mechanical properties of isotropic materials at room temperature

Calorific value	Kcal/Kg^{0}C	0.092	0.052
Modulus of Elasticity	Gpa	110	50
Shear Modulus	GPa	45	18
Poisson Ratio		0.34	0.36
Thermal Expansion coefficient	10 $^{-6}$ m/m^{0}C	17.6	22
Parameters	Units	Copper	Tin
Thermal Conductivity	W/mK	401	66.8
Density	Kg/m^3	8940	5750

For numerical computation, a mixture of Copper (Cu) and Tin (Sn) in the ratio 70:30 is considered. In this regard, Young's modulus is denoted by the expression $E(x) = (0.1174 - 0.2246x + 1.347x^2 - 5.814x^3) \times 9.8\,GPa$. Here $x : (\text{weight of Tin}\%\div 100),\ 0 \leq x \leq 0.3)$. The physical parameters are $\xi_0 = 1$, $\ell = 0.08$ and $T_0 = 150^oC$. In order to examine the influence of heating on the semi-elliptic plate, we performed the numerical calculation and illustrated graphically with the help of MATHEMATICA software.

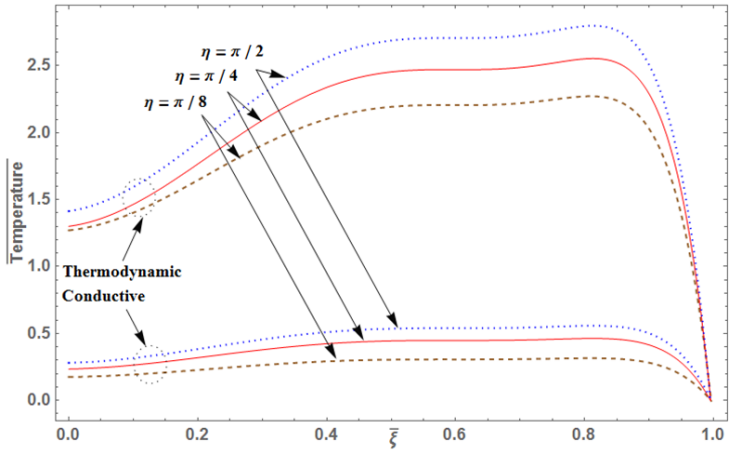

Figure 2. Temperature distribution along the $\bar{\xi}-$ direction for different η

Figure 2 depicts distributions of thermodynamic and conductive temperatures in the $\bar{\xi}$ direction for various values of η. It is clearly noticed from the graph that the effect of the material parameter β is most prominent in thermodynamic temperature distribution. Both temperatures gradually increase up to $\bar{\xi} = 0.4$ then attains the maximum value at the inner core due to tensile forces along the middle part. Further temperature tends to become zero towards the extreme outer end due to the more compressive strength acting towards the outer edges. Both temperature distributions along the angular direction are precisely shown in Figure 3. The temperature distributions attain its maximum value in the neighbourhoods of the center of the heating region along with the η for various time values. It can be seen that the temperature change on the heated surface increases as the thermal

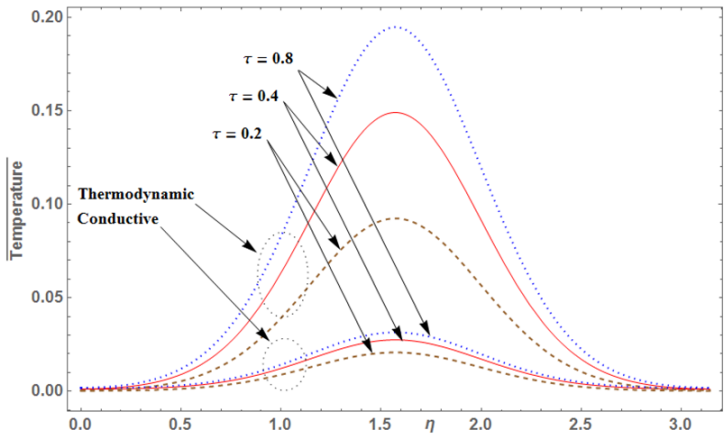

Figure 3. Variation of temperature along the $\eta-$ direction for different time τ

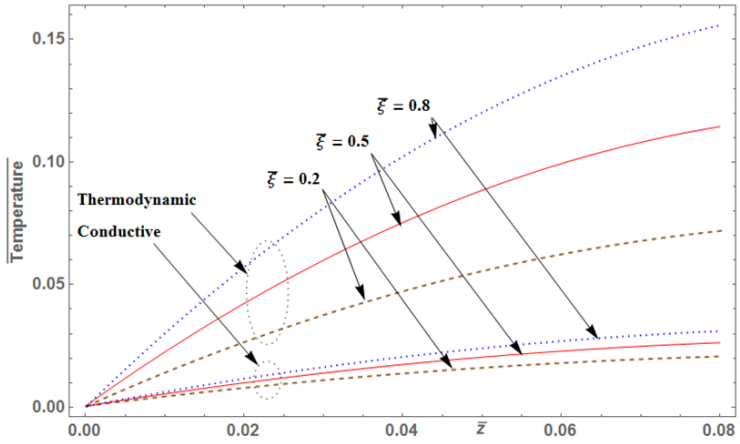

Figure 4. Effect of temperature along the thickness direction for different $\bar{\xi}$

load time is increased. The variation in the thickness direction of the plate is shown in Figure 4. The thermodynamic and conductive temperatures found to be increasing along the $\bar{z}-$ direction for different values of $\bar{\xi}$ due to the available sectional heat supply at $\bar{z} = 0.08$.

In Figure 5, as time proceeds, the temperature distribution gradually increases up to $\tau = 1$ and attains the highest peak and reduces to zero at $\tau = 2.2$ due to the nature of sectional heat supply. As $\tau \to \infty$, the curves follow a sinusoid trend, but the magnitude of crest and trough goes on decreasing. The deflection due to heating according to the Berger method is lower than the Von Kármán method. Figures 6 and 7 show the comparison with the solutions of the Berger and von Kármán equations for large deflection due to the temperature distribution by means of integral transform technique. The results by the Berger equation is denoted by dotted lines and solutions by the Von Kármán equation are shown as dash-dotted lines. The deflection, due to heating according to the Berger method, is lower than the Kármán method, as shown in Figures 6 and 7, and found in agreement with Mizuguchi and Ohnabe (1996). In Figure 6, as time proceeds, the deflection distribution gradually increases from the origin, thus satisfying the initial boundary condition at

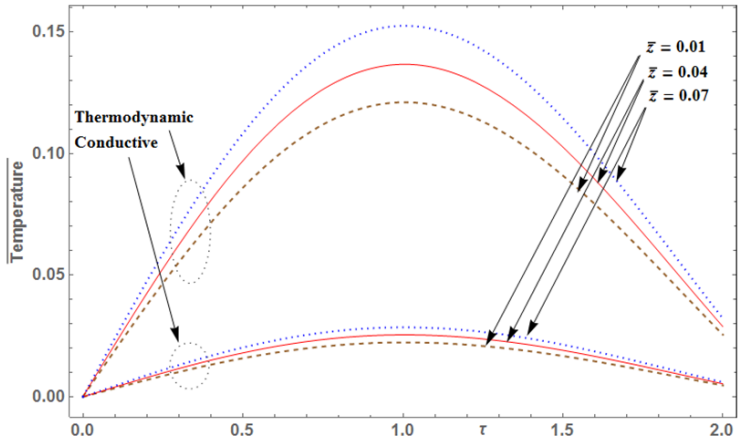

Figure 5. Dimensionless temperature along with the τ trend for different $\bar{z}$

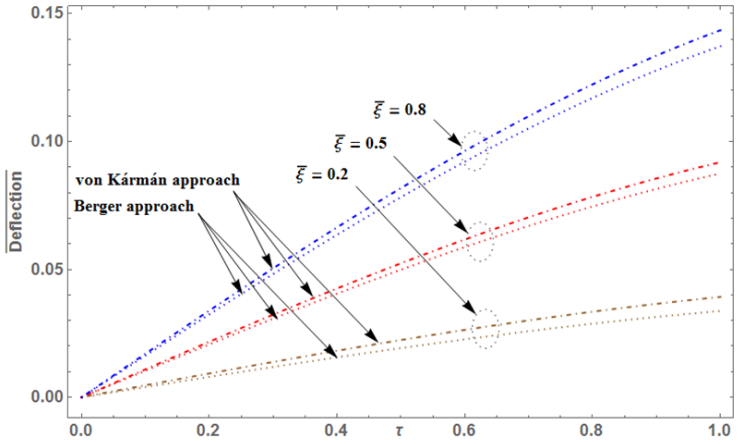

Figure 6. Dimensionless deflection along with the τ trend for different $\bar{\xi}$

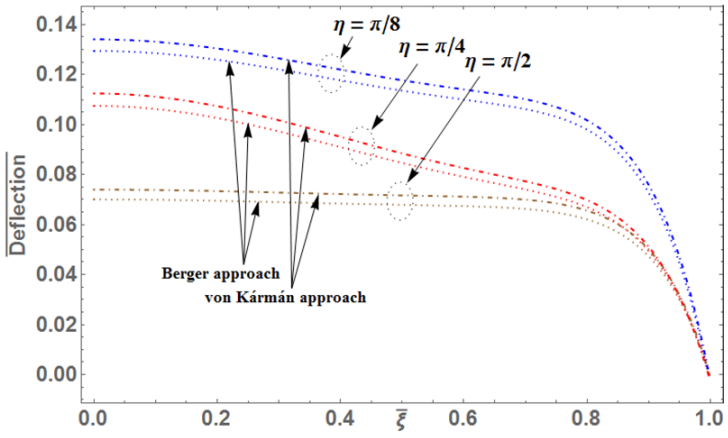

Figure 7. Variation of deflection along the $\bar{\xi}-$ direction for different η

τ. Figure 7 represents the maximum deflection on the middle of the plate, and it also meets the clamped boundary conditions taken in Equation (26).

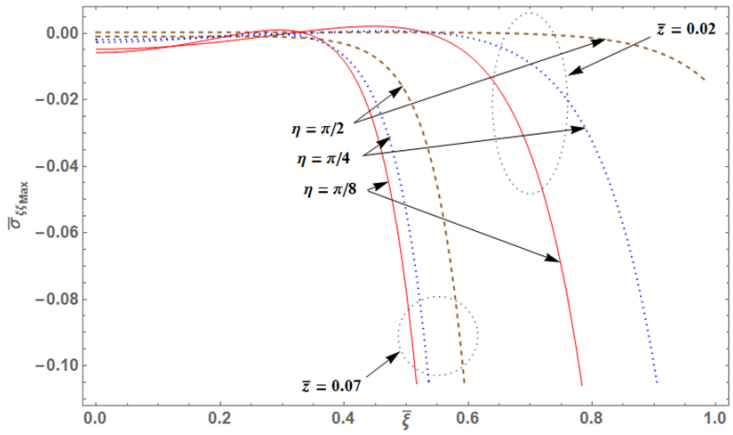

Figure 8. Radial stress distribution along the $\bar{\xi}-$ direction for different η and $\bar{z}$

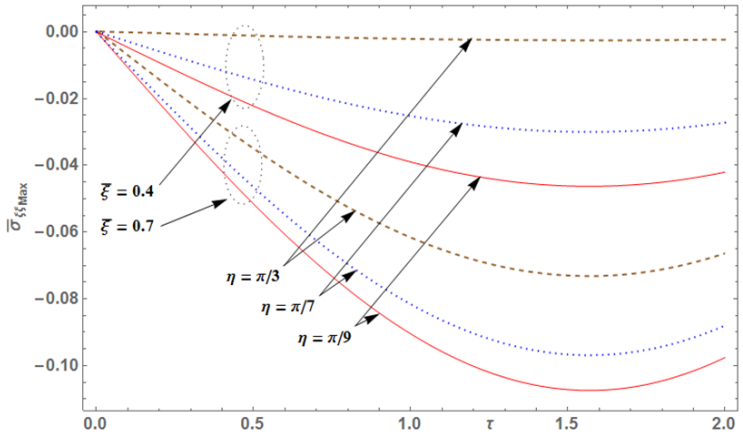

Figure 9. Radial stress distribution along with the time trend τ for different η and $\bar{\xi}$

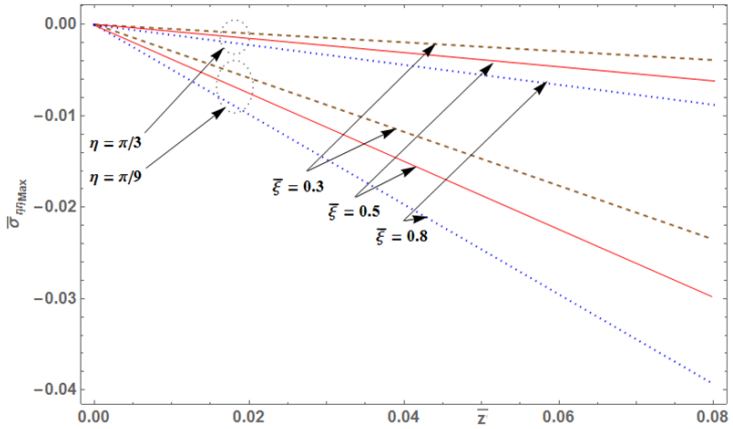

Figure 10. Variation of hoop stress along the $\bar{z}$ direction for a varied $\bar{\xi}$ and η

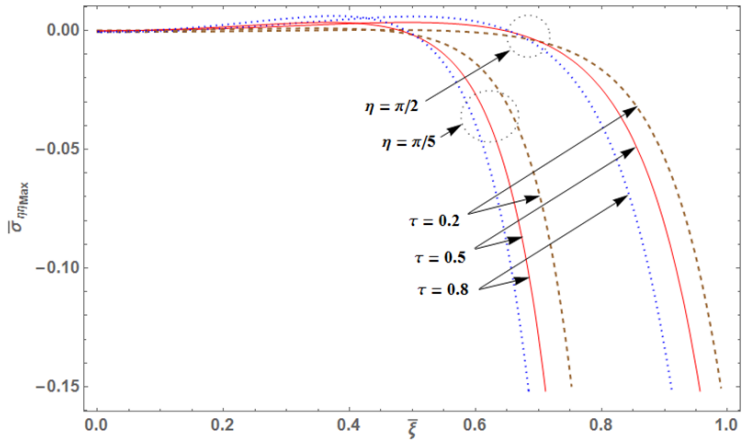

Figure 11. Tangential stress distribution along the $\bar{\xi}-$ direction for different τ and η

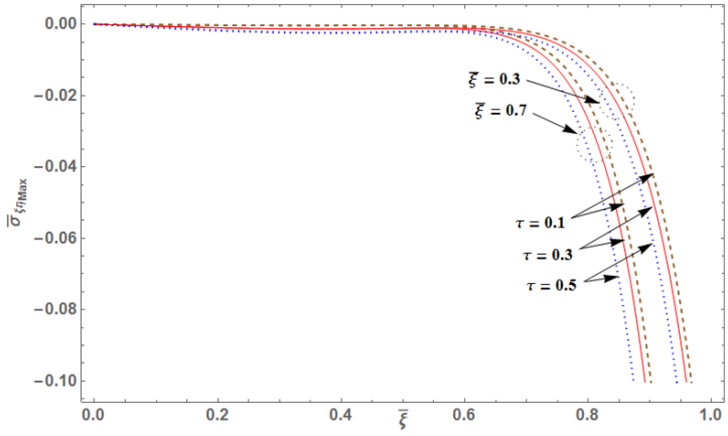

Figure 12. Variation of shear stress along the $\bar{\xi}-$ direction for a varied $\bar{\xi}$ and τ

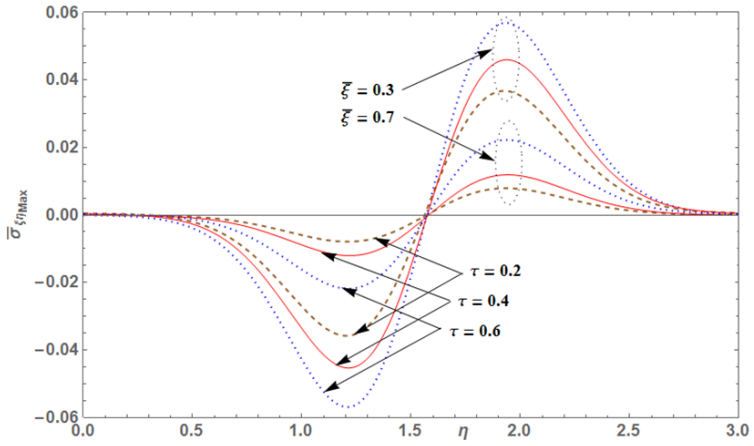

Figure 13. Shear stress distribution along the $\eta-$ direction for different τ and $\bar{\xi}$

Figures 8 through 13 depict the variations of dimensionless thermal bending stresses of the elliptic plate subjected to thermal loading. From Figure 8, it can be seen that the maximum value of tensile stresses occurs up to $\bar{\xi} = 0.4$ along the radial direction, and then the compressive stress acts towards the end. For $\bar{\sigma}_{\xi\xi}$ in Figure 9, as time proceeds the stress distribution gradually decreases is at the lowest at $\tau = 1.6$. Further, it again starts slowly increasing due to the accumulation of energy owing to sectional heat supply.

In Figure 10, it is observed that the tangential stresses linearly decrease along the axial direction for different value of time, and it may be due to the physical thickness. Figure 11 shows that the tensile stresses are maximum at the first part of thickness which is later overlaid by compressive stress at the end along the thickness direction. From Figure 12, it can be seen that the maximum value of the shear stresses occurs up to $\bar{\xi} = 0.6$ along the radial direction, and the compressive stress acts towards the end. In Figure 13, the shear stress distribution shows a sinusoidal nature with two extremes at zero. The interval $(0,\, \pi/2)$ is the region of compressive stresses, and the range $(\pi/2, \pi)$ is the region of tensile stress.

5. Transition to a circular plate

If the elliptic plate degenerates into a circular plate, then θ is independent of η. Then, from McLachlan (1947) $\lambda_{0,m}^2 = \alpha_{0,m}^2/a^2 = \alpha_m^2/a^2 = \lambda_m^2, \alpha_{2n,m}^2 \to p_{0,m}/a^2, m = 0, 1, 2...$ etc. Here $p_{0,m} = p_m$, $p_{0,m}$ being the roots of $J_0(p_{0,m})$. Also $e \to 0$ as $\xi \to \infty$, $\sinh\xi \to \cosh\xi$, $\cosh 2\xi\, d\xi \to 2rdr/h^2$, $A_0^{(0)} \to 2^{-1/2}$, $A_2^{(0)} \to 0$, $\Theta_{2m} \to 0$, $ce_0(\eta, q_{_{0,m}}) \to 2^{-1/2}$, $Ce_0(0, q_{_{0,m}}) \to p_{_0}' J_0(p_{_{0,m}} r)/a$, in which a is the radius of the circular plate and $p_{_0}'$ is constant.

The temperature field in the circular region can be given as

$$T(r,z,t) = \tfrac{1}{2}\sum_{m=1}^{\infty} \tfrac{f(p)}{(\varpi^2 - R_s^2)^{\beta}} \left\{ \tfrac{F(\gamma\,\varpi)}{F(\gamma'\varpi)} \sin(\varpi t) + \sum_{s=1}^{\infty} \left(\tfrac{\pi\varpi}{\varpi^2 - R_s^2} \right) \tfrac{H(R_s)}{M(R_s)} \sin(R_s t) \right\} \times [z + \ell/2]^{(1-m)/2} p_0' J_0(\alpha_m r/a), \tag{57}$$

in which

$$f(p) = \int_0^a r J_0(\alpha_m r/a) f(r) dr.$$

The thermally-induced deflection in the circular region can be denoted as

$$W = \sum_{n=0}^{\infty}\sum_{m=1}^{\infty} A'\ \bar{z}^{(1-m)/2} \left\{ \tfrac{F(\gamma\,\varpi)}{F(\gamma'\varpi)} \sin(\varpi t) + \sum_{s=1}^{\infty} \left(\tfrac{\pi\varpi}{\varpi^2 - R_s^2} \right) \tfrac{H(R_s)}{M(R_s)} \sin(R_s t) \right\} \times Ce_{2n}(\xi, q_{2n,m}) ce_{2n}(\eta, q_{2n,m}), \tag{58}$$

where

$$A' = -\tfrac{1}{2}\sum_{m=1}^{\infty} \tfrac{12\,\alpha_0 E_0 f(p) \ell^{(5-m+4\beta)}\,(-m+1+4\,\beta)}{\ell^3(\varpi^2 - R_s^2)^{\beta}(m-5-4\,\beta)(m-3-4\,\beta)}\, p_0' J_0(\alpha_m r/a)/ \left\langle \{J_0''(\alpha_m r/a)[-1 + (m-1)/2](1-m)\,[z+\ell/2]^{-3-m/2}/2\} - \alpha^2 \{[p_0' J_0(\alpha_m r/a)/2][z+\ell/2]^{(1-m)/2}\} \right\rangle.$$

The author has applied the proposed method in calculating the deflection of a heated semi-circular plate under thermal load with same parameters considered as by Biswas (1976). The comparative

results are illustrated in Table 2, and the results below nearly agrees with the previously given conclusion:

Table 2. Comparison of the proposed results with a previously published paper

α	0.0060	0.0070	0.0080	0.0090
Deflection (Biswas) $\bar{W}$	0.0160	0.0291	0.0301	0.0385
Deflection (Proposed) $\bar{W}$	0.0164	0.0298	0.0323	0.0392

6. Conclusion

In this study, we treated the three-dimensional thermoelastic problem of a medium with nonhomogeneous material properties, such as Young's modulus E, the calorific capacity C_v, the coefficient of linear thermal expansion α_t, and the thermal conductivity k, and with D as varying flexural rigidity as given by Kassir's nonhomogeneity of the axial coordinate variable z.

We successfully established a system of fundamental large deflection equations and its associated bending stresses with an elliptical-cylindrical system utilizing thermal forces and moments. Further, to examine the validity of the proposed method, the elliptic plate degenerated into a circular plate and compared it to those published in the literature. It is also noticed that the assessed results show a strong consensus with those presented in the literature. Moreover, we discussed how these nonhomogeneous material properties affect the temperature distribution, the associated stress distribution and large deflection. Finally, it was also observed that maximum tensile stress arises on the main axis's circular center, contrasting to the elliptical core assumption about the weak heat distribution. This might be owing to insufficient heat penetration through the inner elliptic structure.

Finally, we may conclude that the proposed thermally-induced thermoelastic system can be adapted to other three-dimensional thermoelastic boundary value problems, such as mixed boundary value problems with a penny-shaped crack or traction-free boundary value problems with a moving heat source.

Acknowledgment:

The author(s) are grateful to reviewers, Associate Editor Dr. James R. Valles and Chief Editor Dr. Aliakbar Montazer Haghighi for their valuable suggestions and constructive comments that resulted in the paper being revised to its present form.

REFERENCES

Abd-Alla, A. M., Abd-Alla, A. N. and Zeidan, N. A. (2000). Thermal stresses in a non-homogeneous orthotropic elastic multilayered cylinder, J. Therm. Stress., Vol. 23, pp. 413-428. DOI: 10.1080/014957300403914

Abd-Alla, A. M., El-Naggar, A. M. and Fahmy, M. A. (2003). Magneto-thermoelastic problem in non-homogeneous isotropic cylinder, J. Heat Mass Transf., Vol. 39, pp. 625-629. DOI: 10.1007/s00231-002-0370-3

Agrawal P., Dadheecha P. K., Jat R. N., Bohra M., Nisar K. S. and Khan I. (2020). Lie similarity analysis of MHD flow past a stretching surface embedded in porous medium along with imposed heat source/sink and variable viscosity, J. Materials Research and Technology, Vol. 9, No. 5, pp. 10045-10053. DOI: 10.1016/j.jmrt.2020.07.023

Banerjee, B. and Datta, S. (1979). Large amplitude vibrations of thin elastic plates by the method of conformal transformation, Int. J. Mech. Sci., Vol. 21, pp. 689-696. DOI: 10.1016/0020-7403(79)90048-1

Bhad, P., Varghese, V. and Khalsa, L. (2017). A modified approach for the thermoelastic large deflection in the elliptical plate, Arch. Appl. Mech., Vol. 87, No. 4, pp. 767-781. DOI: 10.1007/s00419-016-1222-9

Biswas, P. (1976). Large deflection of a heated semi-circular plate under stationary temperature distribution, Proc. Net. Inst. Sc., India, Part A, Vol. 83, No. 5, pp. 167-174.

Biswas, P. (1983). Thermal buckling and non-linear free vibrations of polygonal plates at elevated temperature, Proc. 3^{rd} Int. Conf. on Numerical Methods in Thermal Problems, University of Washington, Seattle, USA, Aug. 2-5, pp. 309-319.

Biswas, P. and Kapoor, P. (1984). Non-linear free vibrations and thermal buckling of circular plates at elevated temperature, Indian J. Pure Appl. Math., Vol. 15, No. 7, pp. 809-812.

Buffer, H. (1963a). Die torsion der dicken platte mit stetig veranderlichem schubmodulul, Z. Angew. Math. Mech, Vol. 43, pp. 545-551. DOI: 10.1002/zamm.19630431206

Buffer, H. (1963b). Die torsion der inhomogenen dicken plate, Z. Angew. Math. Mech, Vol. 43, pp. 389-401. DOI: 10.1002/zamm.19630430902

Chen, P. J. and Gurtin, M. E. (1968). On a theory of heat conduction involving two temperatures, Z. Angew. Math. Phys., Vol. 19, No. 4, pp. 614-627. DOI: 10.1007/BF01594969

Chen, P. J., Gurtin, M. E. and Willams W. O. (1969). On the thermodynamics of non-simple elastic material with two temperatures, Z. Angew. Math. Phys., Vol. 20, No. 1, pp. 107-112. DOI: 10.1007/BF01591120

Chiba, R. and Sugano, Y. (2007). Stochastic thermoelastic problem of a functionally graded plate under random temperature load, Arch. Appl. Mech., Vol. 77, pp. 215-227. DOI: 10.1007/s00419-006-0088-7

Ciarletta, M. (1996). Thermoelasticity of non-simple materials with thermal relaxation, J. Therm. Stresses, Vol. 19, No. 8, pp. 731-748. DOI: 10.1080/01495739608946204

Edfawy, E. (2016). Thermal stresses in a non-homogeneous orthotropic infinite cylinder, Struct. Eng. Mech., Vol. 59, No. 5, pp. 841-852. DOI: https://doi.org/10.12989/sem.2016.59.5.841

El-Naggar, A. M., Abd-Alla, A. M., Fahmy, M. A. and Ahmed, S.M. (2002). Thermal stresses in a rotating non-homogeneous orthotropic hollow cylinder, J. Heat Mass Transf., Vol. 39, pp. 41-46. DOI: 10.1007/s00231-001-0285-4

Farhan, A. M., Abd-Alla, A. M. and Khder, M. A. (2019). Solution of a problem of thermal stresses in a non-homogeneous thermoelastic infinite medium of isotropic material by finite difference method, J. Ocean. Eng. Sci., Vol. 4, No. 3, pp. 256-262. DOI: 10.1016/j.joes.2019.05.001

Gupta, R. K. (1964). A finite transform involving Mathieu functions and its application, Proc. Net. Inst. Sc., India, Part A, Vol. 30, No. 6, pp. 779-795.

Hata, T. (1985). Thermal stresses in a nonhomogenous semi-infinite elastic solid under steady distribution of temperature, Trans. Jpn. Soc. Mech. Eng. A., Vol. 51, No. 467, pp. 1789-1794.

Jeon, S. P., Tanigawa, Y. and Sone, D. (1997). Analytical treatment of axisymmetrical thermoelastic field with Kassir's nonhomogeneous material properties and its adaptation to boundary value problem of slab under steady temperature field, J. Therm. Stresses, Vol. 20, No. 3-4, pp. 325-343. DOI: 10.1080/01495739708956105

Kassir, M. K. (1972). Boussinesq problems for nonhomogeneous solid, J. Eng. Mech. Div., Vol. 98, pp. 457-470.

Kassir, M. K. and Sih G. C. (1975). Three-dimensional crack problems, Mechanics of Facture, Leyden: Noordhoff, Vol. 2, pp. 382-409.

Khan, U., Adnan, Ahmed, N., Mohyud-Din S. T., Baleanu, D., Khan, I. and Nisar, K. S. (2020a). A novel hybrid model for Cu-Al2O3/H2O nanofluid flow and heat transfer in convergent/divergent channels, Energies, Vol. 13, pp. 1686. DOI: 10.3390/en13071686

Khan, Z., Rasheed, H. U., Islam, S., Noor, S., Khan, I., Abbas, T., Khan, W., Seikh, A. H., Sherif, E. M. and Nisar, K. S. (2020b). Heat transfer effect on viscoelastic fluid used as a coating material for wire with variable viscosity, Coatings, Vol. 10, pp. 163. DOI: 10.3390/coatings10020163

Manthena, V. R., Lamba, N. K. and Kedar, G. D. (2017). Transient thermoelastic problem of a nonhomogeneous rectangular plate, J. Therm. Stresses, Vol. 40, No. 5, pp. 627-640. DOI: 10.1080/01495739.2016.1237861

McLachlan, N.W. (1947). *Theory and Application of Mathieu Function*, Oxford Univ. Press.

Mizuguchi, F. and Ohnabe H. (1996). Large deflections of heated functionally graded clamped rectangular plates with varying rigidity in thickness direction, Functionally Graded Materials, Elsevier Science, Vol. 2, pp. 81-86.

Nowiski, J.L. (1963). Nonlinear vibrations of elastic circular plates exhibiting rectilinear orthotrophy, Z. Angew. Math. Phys., Vol. 14, pp. 112-124. DOI: 10.1007/BF01589264

Nowinski, J.L. and Ohnabe H. (1972). On certain inconsistencies in Berger equations for large deflections of plastic plates, Int. J. Mech. Sci., Vol. 14, pp. 165-170. DOI: 10.1016/0020-7403(72)90073-2

Ootao, Y. and Tanigawa, Y. (2012). Transient thermoelastic analysis for a multilayered hollow circular disk with piecewise power law nonhomogeneity, J. Therm. Stresses, Vol. 35, No. 1-2, pp. 75-90. DOI: 10.1080/01495739.2012.637749

Pal, M. C. (1970a). Large amplitude free vibration of circular plates subjected to acrodynamic heating, In. J. Soli. Stru., Vol. 6, pp. 301-313, DOI: 10.1016/0020-7683(70)90040-5

Pal, M. C. (1970b). Static and dynamic non-linear behaviour of heated orthotropic circular plates, In. J. Soli. Stru., Vol. 8, pp. 489-504. DOI: 10.1016/0020-7462(73)90040-1

Prathap, G. (1970). On the Berger approximation: a critical re-examination, J. Sound Vibr., Vol. 66, No. 2, pp. 149-154. DOI: 10.1016/0022-460X(79)90661-8

Quintanilla, R. (2003). Thermoelasticity without energy dissipation of non-simple materials, Z. Angew. Math. Mech., Vol. 83, No. 3, pp. 172-180. DOI: 10.1002/zamm.200310017

Quintanilla, R. (2004). On existence, structural stability, convergence and spatial behaviour in thermoelastic with two temperature, Acta Mech, Vol. 168, No. 1-2, pp. 61-73. DOI: 10.1007/s00707-004-0073-6

Sare, H. D. F., Rivera, J. E. M. and Quintanilla, R. (2010). Decay of solutions in non-simple thermoelastic bars, Int. J. Eng. Sci., Vol. 48, pp. 1233-1241. DOI: 10.1016/j.ijengsci.2010.04.014

Sathyamoorthy, M. and Pandalai K. A. V. (1974). Large amplitude vibrations of variable thickness plates, Noise, Shock and Vibration Conf., Monash University, Melbourne, pp. 99-106.

Sutradhar, A., Paulino, G. H. and Gray, L. J. (2002). Transient heat conduction inhomogeneous and non-homogeneous materials by the Laplace transform Galerkin boundary element method, Eng. Anal. Bound. Elem., Vol. 26, No. 2, pp. 119-132. DOI: 10.1016/S0955-7997(01)00090-X

Tanigawa, Y. (1995). Some basic thermoelastic problems for non-homogeneous structural materials, J. Appl. Mech., Vol. 48, pp. 377-389, DOI: 10.1115/1.3005103

Tassaddiq, A., Khan, I. and Nisar, K. S. (2020). Heat transfer analysis in sodium alginate based nanofluid using MoS2 nanoparticles: Atangana-Baleanu fractional model, Chaos, Solitons and Fractals, Vol. 130, pp. 109445. DOI: 10.1016/j.chaos.2019.109445

Zenkour, A. M. and Abouelregal A. E. (2016). Non-simple magneto-thermoelastic solid cylinder with variable thermal conductivity due to harmonically varying heat, Earthq. Struct., Vol. 10, No. 3, pp. 681-697. DOI: 10.12989/eas.2016.10.3.681